Laminar Flow Mass Transfer in a Flat Duct with Permeable Walls

CLARK K. COLTON, KENNETH A. SMITH, PIETER STROEVE, and EDWARD W. MERRILL

Department of Chemical Engineering
Massachusetts Institute of Technology
Cambridge, Massachusetts 02139

SCOPE

Mass transfer rates attainable in separation processes utilizing semipermeable membranes, such as dialysis, ultrafiltration, reverse osmosis, and electrodialysis, are often limited to a major extent by solute transport in the fluid phase. In this paper, a theoretical solution for the concentration profile and mass transfer rate is developed by several techniques for a particularly simple example: fully developed, one-dimensional, laminar flow of a Newtonian fluid between two parallel plates, each of which permits purely diffusive solute transport. The mass flux through the wall is dependent on the wall permeability, and it is this boundary condition which differentiates the problem from the more familiar cases of constant concentration and constant flux at the wall.

The problem is motivated by its application to the dialysis of blood (hemodialysis) for the replacement of kidney function during renal failure. In hemodialysis, the blood flow path may be assumed to be bounded by a composite "wall" composed of a membrane of specified solute permeability bathed in a dialyzate bath of uniform bulk solute concentration and constant mass transfer coefficient. The latter approximation is generally valid when dialyzate flow rate is sufficiently high and the flow regime is turbulent.

The solution to this problem has two immediate uses: prediction of hemodialyzer performance when the relevant transport parameters are known and evaluation of transport parameters, such as membrane permeability or effective solute diffusion coefficient, from measurement of mass transfer performance. Application of the theory developed here to measurement of the effective diffusion coefficient of urea in flowing blood is treated in a subsequent paper.

Previous treatments have dealt largely with the behavior of a nearly fully developed concentration profile and only the first three terms of the series solution have been evaluated. We have obtained higher eigenvalues and have focussed upon transport in the entrance region, where the concentration profile is developing, because of its relevance to the applications cited above. Finally, we have found a simple, approximate technique for estimating the log-mean Sherwood number and mixing cup concentration. This method permits estimates that are well within the accuracy requirements of most engineering problems.

SUMMARY

The first seven eigenvalues, eigenfunctions, and important constants are obtained, using a modified Graetz-type solution, as a function of the dimensionless wall Sherwood number. The latter quantity is proportional to the ratio of the mass transfer resistance in the fluid to that in the wall. The eigenvalues (Figure 1) vary monotonically with wall Sherwood number and fall between the limits associated with the constant concentration ($N_{Sh_w} = \infty$) and constant flux ($N_{Sh_w} = 0$) boundary conditions. Approximate expressions are derived which are asymptotically valid for the higher eigenvalues. The exact and approximate values agree closely for the seventh eigenvalue (Figure 3). The shape of the eigenvalue-wall Sherwood number relationship changes with increases in the number of the eigenvalue, and the value of the higher eigenvalues tends toward that for the constant flux boundary condition.

Overall and fluid-side Sherwood numbers are evaluated for local and log-mean concentration driving forces as a function of dimensionless length and wall Sherwood number. The local fluid-side curves for the constant concentration and constant flux boundary conditions form an envelope between which the curves for finite wall Sherwood number are located (Figure 6). As dimensionless length decreases, these show a perceptible shift towards the constant flux curve, and this behavior is verified within the concentration entrance region by a linear perturbation analysis which constitutes a first-order correction (for finite wall Sherwood number) to the Leveque-type solution for a constant flux boundary condition. As dimensionless length increases from a very low value, the local fluid-side Sherwood number curves for successively lower values of wall Sherwood number "peel off" the constant flux curve.

In contradistinction to this behavior, the curves for the fluid-side, log-mean Sherwood numbers are more nearly parallel (Figure 8). It is shown that, down to small dimensionless lengths, the ratio of the Sherwood number at specified wall Sherwood number to the value for the constant concentration boundary condition, when divided by the same ratio evaluated from the asymptotic values, is nearly unity (Figures 9 and 10). This fortuitous result provides a simple means for calculating the fluid-side, log-mean Sherwood number from the results of the classical Graetz solution and the ratio of the asymptotic Sherwood numbers (Equation (68)). The latter quantity requires knowledge of only the first eigenvalue.

Correspondence concerning this article should be addressed to Prof. Clark K. Colton.

THE PROBLEM

The system considered in this study consists of a dilute solution of constant physical properties which flows in fully developed laminar motion in a semi-infinite flat duct. Concentration is uniform up to a point ($z = 0$) where the fluid contacts a permeable wall, outside of which the concentration is constant. The problem is to find the concentration distribution and mass flux for $z > 0$.

The problem is similar to the classical "Graetz problem" (*1*) which has been studied by a number of investigators (*2, 3*). The system of interest here was first considered by Van der Does de Bye and Schenk (*4*), for the analogous heat transfer problem, and subsequently by Grimsrud and Babb (*5*). Additional efforts with related geometries or boundary conditions have been carried out by Schenk and co-workers (*6* to *10*) and others (*11, 12*). The problem readily reduces to the evaluation of eigenvalues, and prior to this paper only the first three eigenfunctions and eigenvalues have been reported. The importance of obtaining more eigenvalues has been recognized (*3, 13*).

In this study the first seven eigenvalues, eigenfunctions, and important constants are obtained using a modified Graetz-type solution, and asymptotic expressions are derived for higher eigenvalues. Transport behavior in the concentration entrance region is further examined with a perturbation analysis. Finally, an approximate technique for rapidly calculating mass transfer coefficients is developed from the more rigorous results.

ANALYSIS

Assuming steady state conditions, an absence of convection through the wall, homogeneous fluids with no sources or sinks, and a solute partition coefficient of unity between the fluids in the duct and outside the wall, and ignoring axial diffusion which is negligible in the systems of interest (*14*), the problem can be stated in dimensionless form as

$$\frac{3}{2}(1-4y^2)\frac{\partial\theta}{\partial x}=\frac{\partial^2\theta}{\partial y^2} \tag{1}$$

subject to boundary conditions

$$x \leq 0 \quad \text{all } y \quad \theta = 1 \tag{2}$$

$$\text{all } x \quad y = 0 \quad \frac{\partial\theta}{\partial y} = 0 \tag{3}$$

$$\text{all } x \quad y = \frac{1}{2} \quad -\frac{\partial\theta}{\partial y} = N_{Sh_w}\theta \tag{4}$$

The boundary conditions correspond to an initially uniform concentration, symmetry about the center line, and the requirement that the mass flux to the wall equals the mass flux through the wall. The wall Sherwood number N_{Sh_w} was first employed by Grimsrud and Babb (*5*) and is analogous to the wall Nusselt number defined by van der Does de Bye and Schenk (*4*), the ambient side Nusselt number of Schneider (*14*), and the Biot number in transient heat conduction (*15*). It is proportional to the ratio of the mass transfer resistance in the fluid to that in the wall. $N_{Sh_w} = \infty$ is equivalent to a constant concentration boundary condition, and $N_{Sh_w} = 0$ is equivalent to a constant flux boundary condition, as will be shown.

Modified Graetz Solution

By separation of variables, the solution of Equation (1) may be written as

$$\theta = \sum_m A_m Y_m(y) \exp\left(-\frac{2}{3}\beta_m^2 x\right) \tag{5}$$

where β_m and $Y_m(y)$ are the eigenvalues and eigenfunctions, respectively, of

$$\frac{d^2Y}{dy^2} + \beta^2(1-4y^2)Y = 0 \tag{6}$$

with boundary conditions

$$y = 0 \qquad \frac{dY}{dy} = 0 \tag{7}$$

$$y = \frac{1}{2} \qquad -\frac{dY}{dy} = N_{Sh_w}Y \tag{8}$$

Since Equations (6) through (8) constitute a Sturm-Liouville system, A_m is given by

$$A_m = \frac{\int_{-1/2}^{1/2}(1-4y^2)Y_m dy}{\int_{-1/2}^{1/2}(1-4y^2)Y_m^2 dy} \tag{9}$$

The mixing cup concentration is defined by

$$\theta_m = \frac{\int_{-1/2}^{1/2}\theta(1-4y^2)dy}{\int_{-1/2}^{1/2}(1-4y^2)dy} = \sum_m B_m \exp\left(-\frac{2}{3}\beta_m^2 x\right) \tag{10}$$

The definite integrals may be reformulated (*4, 16*) as

$$\int_{-1/2}^{1/2}(1-4y^2)Y_m dy = \frac{2N_{Sh_w}Y_m(1/2)}{\beta_m^2} \tag{11}$$

$$\int_{-1/2}^{1/2}(1-4y^2)Y_m^2 dy = \frac{Y_m^2(1/2)}{\beta_m}\frac{dN_{Sh_w}}{d\beta_m} \tag{12}$$

yielding

$$A_m = \frac{2N_{Sh_w}}{\beta_m Y_m(1/2)\dfrac{dN_{Sh_w}}{d\beta_m}} \tag{13}$$

$$B_m = \frac{6N_{Sh_w}}{\beta_m^3\dfrac{dN_{Sh_w}}{d\beta_m}} \tag{14}$$

Substitution of a power series

$$Y = \sum_n a_n y^n \tag{15}$$

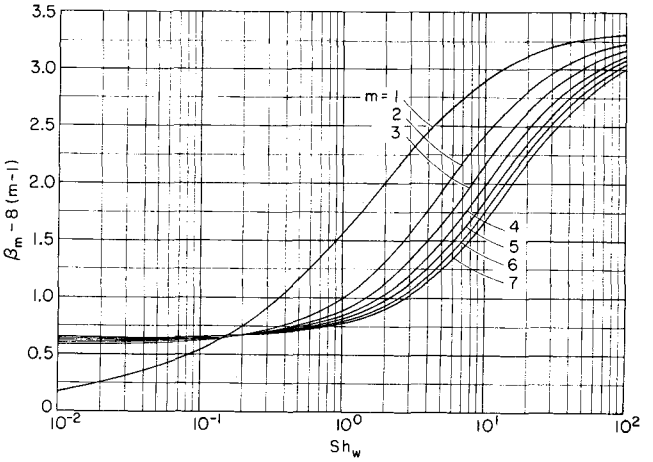

Fig. 1. First seven eigenvalues as a function of wall Sherwood number.

into Equation (6) yields the recurrence relation

$$a_n = \frac{\beta^2}{n(n-1)}\,(4a_{n-4} - a_{n-2}) \qquad (16)$$

with $a_0 = 1$, $a_2 = -\beta^2/2$, and all odd terms equal to zero. The eigenvalues are chosen to satisfy the wall boundary condition, Equation (8), which becomes

$$N_{Sh_w} = -\frac{\sum_n n a_n (\frac{1}{2})^{n-1}}{\sum_n a_n (\frac{1}{2})^n} \qquad (17)$$

from which one obtains

$$\frac{dN_{Sh_w}}{d\beta} = -\frac{\sum_n n \frac{da_n}{d\beta} (\frac{1}{2})^{n-1}}{\sum_n a_n (\frac{1}{2})^n} + \frac{\left[\sum_n n a_n (\frac{1}{2})^{n-1}\right]\left[\sum_n \frac{da_n}{d\beta} (\frac{1}{2})^n\right]}{\left[\sum_n a_n (\frac{1}{2})^n\right]^2} \qquad (18)$$

where

$$\frac{da_n}{d\beta} = \frac{2\beta(4a_{n-4} - a_{n-2}) + \beta^2\left(4\frac{da_{n-4}}{d\beta} - \frac{da_{n-2}}{d\beta}\right)}{n(n-1)} \qquad (19)$$

with $da_0/d\beta = 0$, $da_2/d\beta = -\beta$, and odd terms equal to zero.

The first seven eigenvalues, eigenfunctions, and associated constants were evaluated for 15 values of N_{Sh_w} from 10^{-2} to 10^3, in addition to zero, on a digital computer using 14 significant digits. The simultaneous use of Equations (13), (14), and (15) gave a more rapid and accurate solution (*17*) than the methods employed previously (*4*, *5*). Extensive tabulations of these results, including the eigenvalues, eigenfunctions, and important constants, are available elsewhere (*17*).

In order to evaluate β_m at specified values of N_{Sh_w}, an objective function was defined by

$$F = \left| N_{Sh_w} + \frac{\sum_n n a_n (\frac{1}{2})^{n-1}}{\sum_n a_n (\frac{1}{2})^n} \right| \qquad (20)$$

This converted the calculation to a minimization problem which was solved by a golden section search. Representative eigenvalues are shown in Table 1 and compared with the results of van der Does de Bye and Schenk (*4*) for $N_{Sh_w} = 2$ and 20 and those of Cess and Schaffer (*18*) for the constant flux boundary condition, denoted by λ_m. The results demonstrate the equivalence between λ_{m-1} and β_m for $N_{Sh_w} = 0$.

Figure 1 shows the dependence of the first seven eigen-

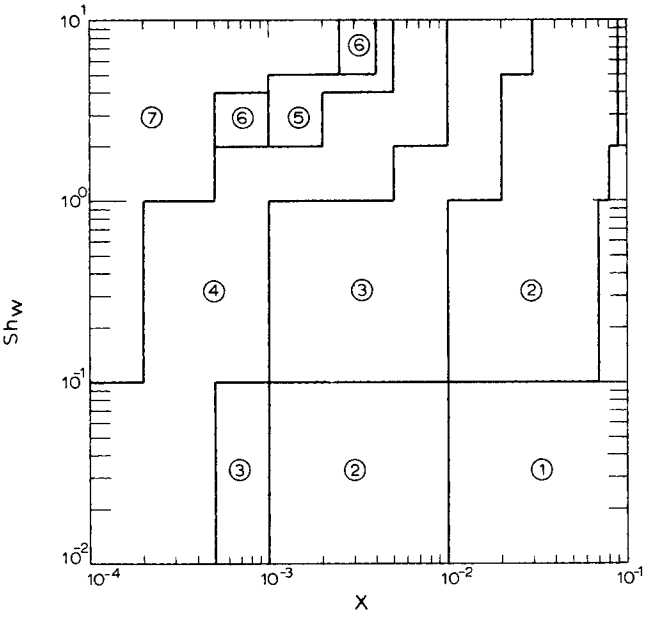

Fig. 2. Number of eigenvalues required for 0.01% accuracy in θ_m as a function of x and N_{Sh_w}. (The limits of the seventh eigenvalue were not evaluated).

Table 1. Eigenvalues for Selected Wall Sherwood Numbers

m	$N_{Sh_w} = \infty$ (3)	$N_{Sh_w} = 100$	$N_{Sh_w} = 20$	$N_{Sh_w} = 20$ ref. (4)	$N_{Sh_w} = 10$	$N_{Sh_w} = 4$
1	3.3631906444	3.30672596	3.1036244	3.1036	2.891947431	2.4402995
2	11.3397146918	11.21496876	10.795510	10.7952	10.410999125	9.7618031
3	19.3364849250	19.16070374	18.605116	18.6050	18.15045572	17.4999650
4	27.3353228852	27.11632948	26.461576		25.974851660	25.35457539
5	35.3347471306	35.07746085	34.346175		33.84564066	33.2600507
6	43.3444106486	43.04235	42.2500		41.7454121	41.19279
7	51.3341929726	51.0090	50.167		49.6642	49.142
8	59.3340420894					
9	67.3339321374					
10	75.3338489126					

m	$N_{Sh_w} = 2$	$N_{Sh_w} = 2$ ref. (4)	$N_{Sh_w} = 1$	$N_{Sh_w} = 0.1$	$N_{Sh_w} = 0$	Const. flux bound. cond. λ_m, ref. (18)
1	2	2	1.55101554	0.54117720	0	8.57448
2	9.312275	9.3124	8.9917222	8.62144383	8.57444987	16.60744
3	17.124040	17.1236	16.88626094	16.63733279	16.60744896	24.6228
4	25.031677		24.83852812	24.64408443	24.62121211	
5	32.975297		32.81042639	32.6479490	32.62904341	
6	40.9367		40.791589	40.650510	40.6342	
7	48.908		48.7779	48.6522	48.638	

values on the wall Sherwood number. The first eigenvalue displays a shape significantly different from the others because it goes to zero at $N_{Sh_w} = 0$. The number of terms required in the power series increases for higher eigenvalues, and round-off error prevented evaluation of more than the first seven eigenvalues.

The number of eigenvalues required for 0.01% accuracy in θ_m is shown in Figure 2 as a function of x and N_{Sh_w}. For $5 \leq N_{Sh_w} \leq \infty$, the criteria remain constant. Below $N_{Sh_w} = 10^{-2}$, two eigenvalues are required for $10^{-4} < x < 10^{-3}$ and four for $10^{-5} < x < 10^{-4}$. The limits of the seventh eigenvalue were not evaluated. By perturbing the eigenvalues from their true values, the accuracy requirement to meet the above criterion for θ_m was found to be about one part in 20,000 to 50,000 for the eigenvalues.

Routine evaluation of more than two eigenvalues by minimizing Equation (20) used prohibitive amounts of computer time. For this purpose, the curves shown in Figure 1 were evaluated on transformed coordinates and fitted by high-order polynomials. The eigenvalues evaluated by this means satisfied the accuracy criterion for $N_{Sh_w} > 10^{-2}$ and $m > 2$. The functional form and coefficients of these polynomials are described elsewhere (*16*).

Asymptotic Expressions

The difficulty of evaluating the higher eigenvalues and eigenfunctions provides motivation for deriving asymptotic expressions for these quantities. For large β and y close to one-half, Sellars, Tribus, and Klein (*13, 18*) showed that the solution to Equation (6) is given by

$$Y(\eta) = \frac{2}{3}\left(\frac{\beta\pi\eta}{2}\right)^{1/2}\left[\sin\left(\frac{\beta\pi}{8}-\frac{\pi}{12}\right)J_{1/3}\left(\frac{\beta\sqrt{8}}{6}\eta^{3/2}\right) - \sin\left(\frac{\beta\pi}{8}-\frac{5\pi}{12}\right)J_{-1/3}\left(\frac{\beta\sqrt{8}}{6}\eta^{3/2}\right)\right] \quad (21)$$

where $\eta = 1 - 2y$. This leads to

$$Y|_{\eta=0} = Y|_{y=1/2} = -\left(\frac{2}{3}\right)^{2/3}\frac{\pi^{1/2}}{\Gamma\left(\frac{2}{3}\right)}\beta^{1/6}\sin\left(\frac{\beta\pi}{8}-\frac{5\pi}{12}\right)$$

$$= -0.998905\,\beta^{1/6}\sin\left(\frac{\beta\pi}{8}-\frac{5\pi}{12}\right) \quad (22)$$

$$\left.\frac{dY}{d\eta}\right|_{\eta=0} = -\frac{1}{2}\left.\frac{dY}{dy}\right|_{y=1/2} = \frac{2^{1/3}\pi^{1/2}}{3^{4/3}\Gamma\left(\frac{4}{3}\right)}\beta^{5/6}\sin\left(\frac{\beta\pi}{8}-\frac{\pi}{12}\right)$$

$$= 0.577983\,\beta^{5/6}\sin\left(\frac{\beta\pi}{8}-\frac{\pi}{12}\right) \quad (23)$$

Satisfaction of the wall boundary condition, Equation (8), requires

$$N_{Sh_w} = -\left(\frac{2}{3}\right)^{2/3}\frac{\Gamma\left(\frac{2}{3}\right)}{\Gamma\left(\frac{4}{3}\right)}\frac{\sin\left(\frac{\beta\pi}{8}-\frac{\pi}{12}\right)}{\sin\left(\frac{\beta\pi}{8}-\frac{5\pi}{12}\right)}\beta^{2/3}$$

$$= -1.157233\,\beta^{2/3}\frac{\sin\left(\frac{\beta\pi}{8}-\frac{\pi}{12}\right)}{\sin\left(\frac{\beta\pi}{8}-\frac{5\pi}{12}\right)} \quad (24)$$

Differentiation of Equation (24) and rearrangement yields

$$\frac{dN_{Sh_w}}{d\beta} = N_{Sh_w}\left[\frac{2}{3\beta} - \frac{\pi\sqrt{3}}{8\left(\frac{1}{2}-\sin\frac{\beta\pi}{4}\right)}\right] \quad (25)$$

Finally, combining these results with Equations (13) and (14) gives

$$A_m = -\frac{2\sin\left(\frac{\beta\pi}{8}-\frac{\pi}{12}\right)}{\frac{2^{2/3}\pi^{1/2}}{3^{5/3}\Gamma\left(\frac{2}{3}\right)}\beta^{1/2}\left(\frac{1}{2}-\sin\frac{\beta\pi}{4}\right) - \frac{\pi^{3/2}}{2^{10/3}(3^{1/6})\Gamma\left(\frac{2}{3}\right)}\beta^{7/6}}$$

$$= -\frac{\sin\left(\frac{\beta\pi}{8}-\frac{\pi}{12}\right)}{0.166484\,\beta^{1/6}\left(\frac{1}{2}-\sin\frac{\beta\pi}{4}\right) - 0.169858\,\beta^{7/6}} \quad (26)$$

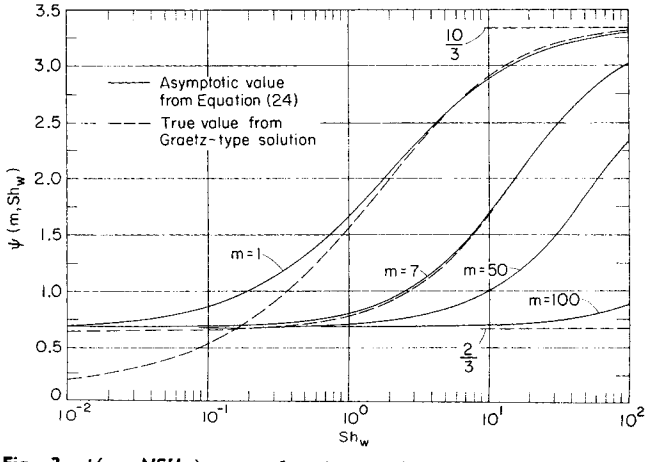

Fig. 3. $\psi(m, NSH_w)$ as a function of N_{Sh_w} for various values of m.

TABLE 2. FIRST SEVEN EIGENVALUES EVALUATED FROM ASYMPTOTIC EXPRESSION, EQUATION (24)

m	$N_{Sh_w} = 1$	$N_{Sh_w} = 4$	$N_{Sh_w} = 20$
1	1.655	2.452	3.080
2	9.062	9.795	10.795
3	16.936	17.53[1]	18.609
4	24.879	25.382	26.467
5	32.845	33.285	34.352
6	40.822	41.216	42.257
7	48.805	49.163	50.175

$$B_m = \frac{6}{\beta^3\left[\frac{2}{3\beta} - \frac{\pi\sqrt{3}}{8\left(\frac{1}{2} - \sin\frac{\beta\pi}{4}\right)}\right]} \quad (27)$$

Eigenvalues were evaluated from Equation (24) by minimization of an objective function defined analogously to Equation (20). Representative results for the first seven eigenvalues are shown in Table 2 for $N_{Sh_w} = 1$, 4, and 20. Comparison with the results of Table 1 show reasonable agreement, even at moderate values of β_m. Hence, it can be concluded that, for most problems of practical interest, all the eigenvalues for this problem are now sufficiently accurately known.

Examination of Equation (24) shows that

$$\beta_m = 8(m-1) + \frac{10}{3} \quad (28)$$

for $N_{Sh_w} = \infty$ and

$$\beta_m = 8(m-1) + \frac{2}{3} \quad (29)$$

for $N_{Sh_w} = 0$. This is in accord with previous results for the constant concentration and constant flux boundary conditions, respectively (*13, 18*). For intermediate values of N_{Sh_w}, the eigenvalues may be represented by

$$\beta_m = 8(m-1) + \psi(m, N_{Sh_w}) \quad (30)$$

where $2/3 \leq \psi(m, N_{Sh_w}) \leq 10/3$.

Figure 3 shows the dependence of $\psi(m, N_{Sh_w})$ on N_{Sh_w} for $m = 1$, 7, 50 and 100 and a comparison with the true values obtained from the modified Graetz solution for $m = 1$ and 7 (taken from Figure 1). Agreement between the true values and the asymptotic expression is best at higher N_{Sh_w} and decreases with decreasing N_{Sh_w}. Contrary to the postulate of van der Does de Bye and Schenk (*4*), it is clear that the shape of the $\beta_m - N_{Sh_w}$ relationship continues to change for modest values of m. However, as m becomes very large, successive eigenvalues do in fact differ by a constant and $\psi(m, N_{Sh_w})$ tends toward the constant flux value, 2/3. This may be seen by rearranging Equation (24)

$$\frac{\sin\left(\frac{\beta\pi}{8} - \frac{\pi}{12}\right)}{\sin\left(\frac{\beta\pi}{8} - \frac{5\pi}{12}\right)} \propto \frac{N_{Sh_w}}{\beta^{2/3}} \quad (31)$$

As $\beta \to \infty$, the right-hand side tends to zero (unless $N_{Sh_w} \to \infty$), which leads to Equation (29) and thus $\psi(m, N_{Sh_w}) \to 2/3$.

Perturbation Solution

When x is small, a large number of terms must be used in the modified Graetz solution, Equation (5). For this case, a Leveque-type solution is a good approximation. Assuming a linear velocity profile within the concentration boundary layer, the problem becomes

$$6\omega\frac{\partial\theta}{\partial x} = \frac{\partial^2\theta}{\partial\omega^2} \quad (32)$$

with boundary conditions

$$x \leq 0 \qquad \text{all } \omega \qquad \theta = 1 \quad (33)$$

$$\text{all } x \qquad \omega = \infty \qquad \theta = 1 \quad (34)$$

$$\text{all } x \qquad \omega = 0 \qquad \frac{\partial\theta}{\partial\omega} = N_{Sh_w}\theta \quad (35)$$

A solution is sought of the form

$$\theta - 1 = \epsilon f_1(\xi) + \epsilon^2 f_2(\xi) + \epsilon^3 f_3(\xi) + \ldots = \sum_n \epsilon^n f_n(\xi) \quad (36)$$

valid for $\epsilon << 1$, where

$$\epsilon = 6^{-1/3} N_{Sh_w} x^{1/3} \quad (37)$$

and ξ is the similarity transformation variable employed by Leveque (*19*),

$$\xi = 6^{1/3}\,\omega x^{-1/3} \quad (38)$$

The problem reduces to finding the functions $f_n(\xi)$. Using the first two terms of Equation (36) and substituting into Equation (32) gives, after rearrangement,

$$\left[f_1'' + \frac{1}{3}\xi^2 f_1' - \frac{1}{3}\xi f_1\right] + \epsilon\left[f_2'' + \frac{1}{3}\xi^2 f_2' - \frac{2}{3}\xi f_2\right] = 0 \quad (39)$$

where primes denote differentiation with respect to ξ. Requiring that coefficients of powers of ϵ independently go to zero yields

$$f_1'' + \frac{1}{3}\xi^2 f_1' - \frac{1}{3}\xi f_1 = 0 \quad (40)$$

$$f_2'' + \frac{1}{3}\xi^2 f_2' - \frac{2}{3}\xi f_2 = 0 \quad (41)$$

with boundary conditions

$$f_1(\infty) = f_2(\infty) = 0 \quad (42, 43)$$

From the third boundary condition, Equation (35), one obtains

$$[f_1'(0) - 1] + \epsilon[f_2'(0) - f_1(0)] + O[\epsilon^2] = 0 \quad (44)$$

As above, setting the terms in brackets equal to zero yields

$$f_1'(0) = 1 \qquad f_2'(0) = f_1(0) \quad (45, 46)$$

Equation (40) may be transformed into

$$\xi f_1''' + \left(\frac{1}{3}\xi^3 - 1\right) f_1'' = 0 \quad (47)$$

Defining

$$\chi = 9^{-1/3}\xi \quad (48)$$

$$Q(\chi) = f_1' \quad (49)$$

yields

$$\chi Q'' + (3\chi^3 - 1)Q = 0 \quad (50)$$

with

$$\chi = 0 \qquad Q = 1 \quad (51)$$

$$\chi = \infty \qquad Q = 0 \quad (52)$$

This is the equation obtained by Bird (*20*) for the entrance region with a constant flux boundary condition, for which the solution is

$$Q = \frac{\Gamma\left(\frac{2}{3}, \chi^3\right)}{\Gamma\left(\frac{2}{3}\right)} \quad (53)$$

and

$$f_1 = -9^{1/3}\left[\frac{e^{-\chi^3}}{\Gamma\left(\frac{2}{3}\right)} - \chi\left\{1 - \frac{\Gamma\left(\frac{2}{3}, \chi^3\right)}{\Gamma\left(\frac{2}{3}\right)}\right\}\right] \quad (54)$$

Hence, $f_1(0) = -9^{1/3}/\Gamma\left(\frac{2}{3}\right) \cong -1.5361$

The analogy with Bird's formulation may be seen by defining a dimensionless concentration using only the f_1 term in Equation (36)

$$\frac{\theta - 1}{N_{Sh_w}} = 6^{-1/3}\, x^{1/3} f_1(\xi) \qquad (55)$$

It is clear that the f_1 term alone corresponds to a Leveque-type solution for a flat duct with a constant flux at the wall given by $k_w(c_i - c_0)$. Hence, the f_2 term is a first-order correction to the constant flux solution for finite, non-zero N_{Sh_w}. Consequently, as x approaches zero, all solutions for finite N_{Sh_w} approach that of the constant flux boundary conditions.

Equation (41) was solved numerically on a digital computer using Hammings' modified predictor-corrector method (*16*) by successively guessing $f_2(0)$ until Equation (43) was satisfied to within $\pm\ 10^{-4}$ at $\xi = 25$. The solutions for both f_1 and f_2 are shown in Figure 4. $f_2(0)$ was determined to be 2.0842.

DISCUSSION

The Sherwood numbers of interest may be calculated directly from the modified Graetz solution described above. The local overall Sherwood number is obtained from

$$N_{Sh_o} = -\frac{1}{\theta_m}\left(\frac{\partial\theta}{\partial y}\right)_{y=1/2} = -\frac{1}{2\theta_m}\left(\frac{d\theta_m}{dx}\right) \qquad (56)$$

$N_{Sh_o} = N_{Sh_w}$ at $x = 0$, and it decreases with increasing x to an asymptotic value $N_{Sh_o}(x \to \infty)$, equal to $\frac{1}{3}\beta_1^2$.

The local fluid-side Sherwood number is given by

$$N_{Sh_f} = -\frac{1}{(\theta_m - \theta_w)}\left(\frac{\partial\theta}{\partial y}\right)_{y=1/2} \qquad (57)$$

From additivity of resistances, an equivalent expression yielding identical results is

$$\frac{1}{N_{Sh_o}} = \frac{1}{N_{Sh_w}} + \frac{1}{N_{Sh_f}} \qquad (58)$$

Figure 5 shows the dependence of the asymptotic local fluid-side Sherwood number on wall Sherwood number, as well as the ratio $\phi(N_{Sh_w})$, between N_{Sh_f} at finite N_{Sh_w} and the value for $N_{Sh_w} = \infty$.

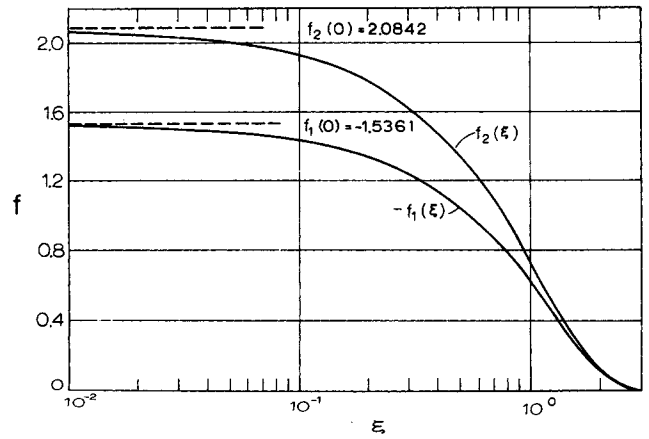

Fig. 4. f_1 and f_2 as a function of ξ.

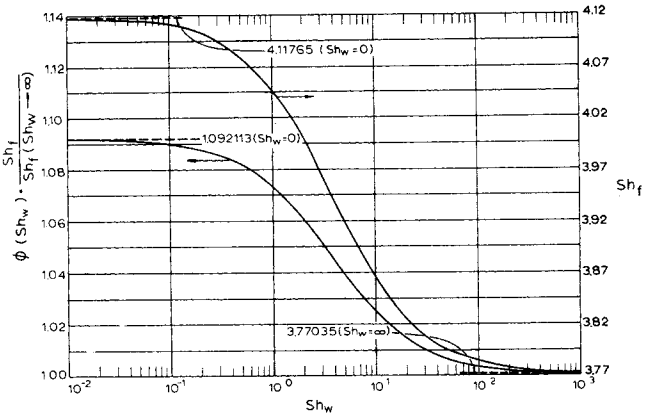

Fig. 5. Limiting ($x \to \infty$) fluid-side Sherwood number and $\phi(N_{Sh_w})$ as a function of N_{Sh_w}.

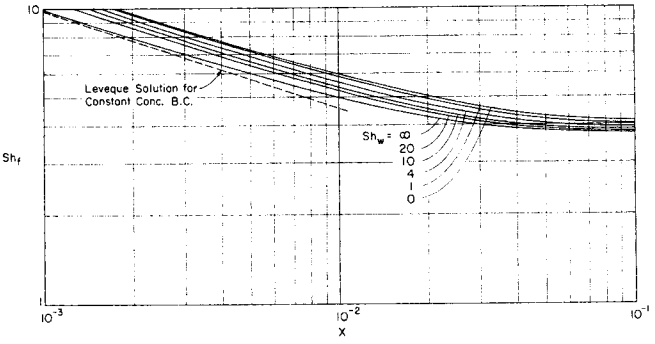

Fig. 6. Local fluid-side Sherwood number as a function of dimensionless length and wall Sherwood number.

Local fluid-side Sherwood numbers as a function of x are shown for various N_{Sh_w} in Figure 6. The constant concentration ($N_{Sh_w} = \infty$) and constant flux ($N_{Sh_w} = 0$) curves form an envelope between which the curves for finite N_{Sh_w} are located. The asymptotic values are encompassed by the limits shown in Figure 5, which have a ratio of 1.0921. At small values of x (less than shown in Figure 6), the bounding curves are given by the Leveque solution for boundary conditions of constant concentration

$$N_{Sh}(N_{Sh_w} = \infty) = \frac{3}{\Gamma\left(\frac{1}{3}\right)}\left(\frac{2}{3}\right)^{1/3} x^{-1/3} = 0.97828x^{-1/3} \qquad (59)$$

and constant flux

$$N_{Sh}(N_{Sh_w} = 0) = \left(\frac{2}{3}\right)^{1/3}\Gamma\left(\frac{2}{3}\right) x^{-1/3} = 1.1829x^{-1/3} \qquad (60)$$

which have a ratio of 1.2092.

It is clear from Figure 6 that the curves for finite N_{Sh_w} are not parallel, neither to themselves nor to either limiting case. As x decreases, there is a small but perceptible shift towards the constant flux curve. The behavior in the entrance region may be further examined using the perturbation solution. Noting that for a Leveque-type solution, $\theta_m \simeq 1$, the local overall Sherwood number is given by

$$N_{Sh_o} = \left(\frac{\partial\theta}{\partial\omega}\right)_{\omega=0} = N_{Sh_w}\left[1 - \frac{6^{-1/3}(9^{1/3})}{\Gamma\left(\frac{2}{3}\right)} N_{Sh_w} x^{1/3}\right]$$

$$= N_{Sh_w}\left[1 - 0.8453\, N_{Sh_w} x^{1/3}\right] \qquad (61)$$

As expected, $N_{Sh_o} \to N_{Sh_w}$ as $x \to 0$. The fluid-side relation becomes

$$N_{Sh_f} = \frac{1}{1-\theta_w}\left(\frac{\partial\theta}{\partial\omega}\right)_{\omega=0}$$

$$= 6^{1/3}x^{-1/3}\left[\frac{1-\dfrac{6^{-1/3}(9^{1/3})}{\Gamma\left(\frac{2}{3}\right)}N_{Sh_w}x^{1/3}}{\dfrac{9^{1/3}}{\Gamma\left(\frac{2}{3}\right)}-6^{-1/3}f_2(0)N_{Sh_w}x^{1/3}}\right]$$

$$= 1.817x^{-1/3}\left[\frac{1-0.8453\,N_{Sh_w}x^{1/3}}{1.5361-1.147\,N_{Sh_w}x^{1/3}}\right] \quad (62)$$

Rearranging Equation (62), approximating $\dfrac{1}{1+\epsilon}$ as $1-\epsilon$ for $\epsilon << 1$, and dropping terms of order ϵ^2 yields

$$N_{Sh_f} \cong \left(\frac{2}{3}\right)^{1/3}\Gamma\left(\frac{2}{3}\right)x^{-1/3}$$

$$\left[1+6^{-1/3}N_{Sh_w}x^{1/3}\left[\frac{f_2(0)\Gamma\left(\frac{2}{3}\right)}{9^{1/3}}-\frac{9^{1/3}}{\Gamma\left(\frac{2}{3}\right)}\right]\right]$$

$$= 1.1829x^{-1/3} - 0.1320\,N_{Sh_w} \quad (63)$$

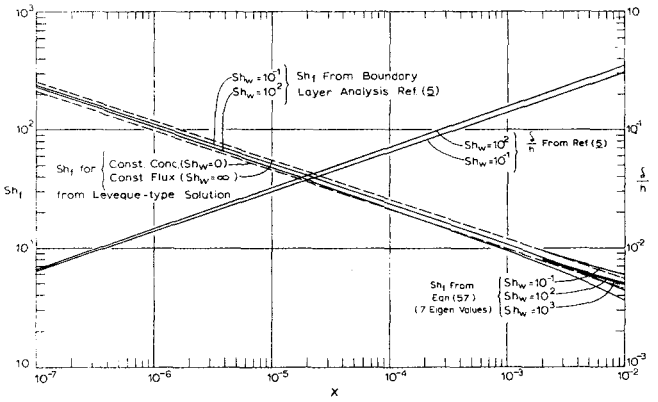

Fig. 7. Entrance region solutions for local fluid-side Sherwood number.

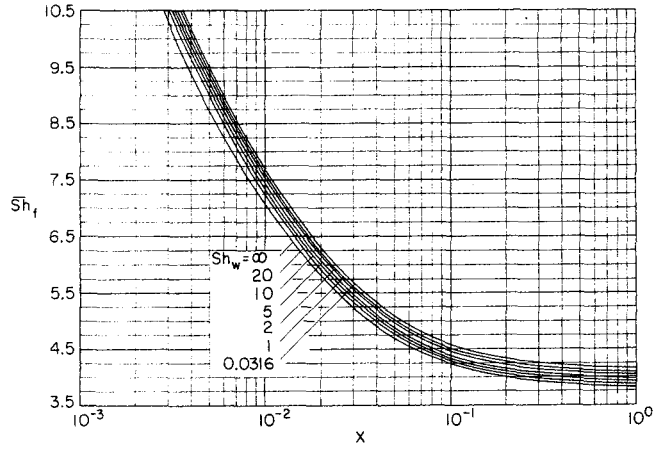

Fig. 8. Log-mean, fluid-side Sherwood number as a function of dimensionless length and wall Sherwood number.

Equation (63) demonstrates two interesting results. First, for $N_{Sh_w} = 0$, N_{Sh_f} is given by the first term which represents the Leveque solution for a constant flux boundary condition. Secondly, as x increases from a very low value, N_{Sh_f} for successively lower values of N_{Sh_w} will "peel off" the constant flux curve. This is consistent with the shift in the N_{Sh_f} curves noted on Figure 6 and with the behavior of the larger eigenvalues illustrated in Figure 3.

Grimsrud and Babb (5) obtained an alternative entrance region solution by an approximate integral boundary layer technique and reported their results in terms of N_{Sh_o} and a concentration boundary layer thickness δ. Their analysis was reformulated (16) to compare with the results of this study, and a representative summary is shown in Figure 7. The estimate of N_{Sh_f} fails to approach the constant flux Leveque solution at low x; and, at $x = 2 \times 10^{-3}$, the boundary layer solution deviates considerably from the results of the eigenvalue solution. Hence, attempting to match the boundary layer analysis with the eigenvalue solution at this value or at higher values of x will lead to erroneous results. Integral boundary layer analyses are most effective if the scalar profile is self-similar in terms of some appropriate variable. In the present case, such a similarity transformation does not exist and the solution of Grimsrud and Babb is therefore somewhat inaccurate, especially as their polynomial approximation to the concentration profile contained only three terms.

The perturbation solution for $N_{Sh_w} = 10^{-1}$ gives a curve which is not visually different from the constant flux line. This means that, for low N_{Sh_w}, the effect of a parabolic velocity profile becomes important before the influence of the non-zero N_{Sh_w} becomes apparent. For $N_{Sh_w} = 10^2$, the perturbation analysis is not valid within the plotted range of x.

For the analysis of practical mass transfer devices, mass transfer coefficients based upon the logarithmic mean concentration difference are of more general utility. The log-mean, overall Sherwood number, defined by

$$\overline{N}_{Sh_o} = \frac{1}{x}\int_0^x N_{Sh_o}dx = \frac{1}{2x}\ln\left(\frac{1}{\theta_m}\right) \quad (64)$$

may be calculated directly from the solution for θ_m. The log-mean, fluid-side Sherwood number may be obtained from a relation analogous to Equation (58)

$$\frac{1}{\overline{N}_{Sh_o}} = \frac{1}{N_{Sh_w}} + \frac{1}{\overline{N}_{Sh_f}} \quad (65)$$

Figure 8 contains a plot of $\overline{N}_{Sh_f}$ as a function of x for various values of N_{Sh_w}. In contradistinction to the results for N_{Sh_f}, the $\overline{N}_{Sh_f}$ curves are roughly parallel and show a much less significant shift away from the curve for $N_{Sh_w} = \infty$ over the range plotted. This behavior is somewhat surprising, although the relationship between $\overline{N}_{Sh_f}$ and N_{Sh_f} is complex, as can be seen by combining Equations (58), (64), and (65) to give

$$\overline{N}_{Sh_f} = N_{Sh_w}\left[\frac{\dfrac{1}{x}\displaystyle\int_0^x \frac{N_{Sh_f}}{N_{Sh_w}+N_{Sh_f}}dx}{1-\dfrac{1}{x}\displaystyle\int_0^x \frac{N_{Sh_f}}{N_{Sh_w}+N_{Sh_f}}dx}\right] \quad (66)$$

The unexpected behavior of $\overline{N}_{Sh_f}$ fortuitously permits an approximate but accurate method for estimating $\overline{N}_{Sh_o}$ and hence θ_m. Figures 9 and 10 contain plots of $\phi'(x, N_{Sh_w})$, defined by

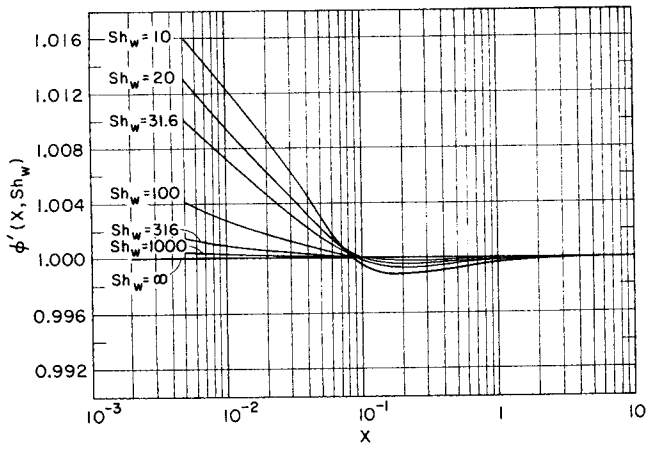

Fig. 9. $\phi'(x, N_{Sh_w})$ as a function of x for various values of N_{Sh_w}.

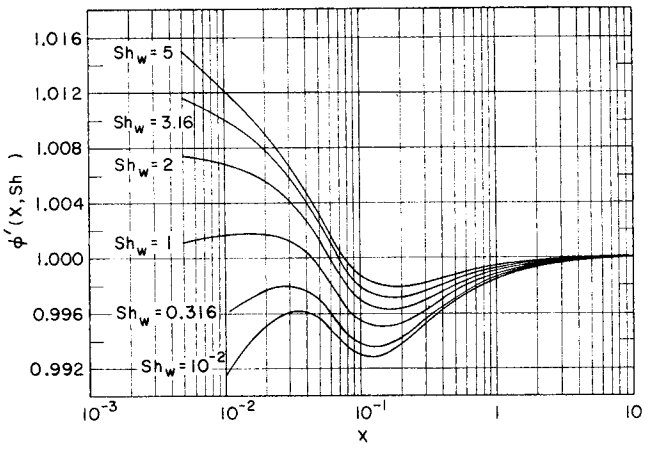

Fig. 10. $\phi'(x, N_{Sh_w})$ as a function of x for various values of N_{Sh_w}.

$$\phi'(x, N_{Sh_w}) = \frac{\overline{N}_{Sh_f}/\overline{N}_{Sh_f}(N_{Sh_w} = \infty)}{\phi(N_{Sh_w})} \qquad (67)$$

where $\phi(N_{Sh_w})$ is given in Figure 5. Over the entire range of N_{Sh_w} studied, $\phi'(x, N_{Sh_w})$ is within about one percent of unity for $x > 5 \times 10^{-3}$. Hence, $\overline{N}_{Sh_f}$ may be approximated by

$$\overline{N}_{Sh_f} = \phi(N_{Sh_w})\, \overline{N}_{Sh_f}\,(N_{Sh_w} = \infty) \qquad (68)$$

and used in Equation (65) to calculate $\overline{N}_{Sh_o}$. By this means, the desired parameters may be evaluated using the results of the classical Graetz solution without calculating the eigenvalues. This technique was tested for various combinations of x and N_{Sh_w} and was found to yield an accuracy in θ_m of 0.3% or better.

ACKNOWLEDGMENTS

This study was supported in part by Contract PH 43-66-491 from the National Institute of Arthritis and Metabolic Diseases, NIH, USPHS, by an NIH Predoctoral Fellowhip to C. K. Colton and by an NSF traineeship to P. Stroeve.

NOTATION

A_m = coefficient in Equation (5)
a_n = power series coefficient in Equation (15)
B_m = coefficient in Equation (10)
c = concentration
D = diffusion coefficient
F = objective function defined in Equation (20)
f = function of ξ, defined by Equation (36)
h = channel height
$J_p(x)$ = Bessel function of the first kind of order p
k = local mass transfer coefficient
$\overline{k}$ = logarithmic mean mass transfer coefficient
k_w = wall mass transfer coefficient
r = transverse coordinate
Q = quantity defined by Equation (49)
N_{Sh} = local Sherwood number, kh/D
$\overline{N}_{Sh}$ = logarithmic mean Sherwood number, $\overline{k}\,h/D$
N_{Sh_w} = wall Sherwood number, $k_w h/D$
$\overline{v}$ = mean velocity
x = dimensionless coordinate, $zD/\overline{v}\,h^2$
Y = eigenfunction
y = dimensionless coordinate, r/h
z = axial coordinate

Greek Letters

β = eigenvalue
$\Gamma(a)$ = gamma function
$\Gamma(a, b)$ = incomplete gamma function
δ = concentration boundary layer thickness
ϵ = quantity defined by Equation (37)
η = dimensionless coordinate, $1 - 2y$
λ = eigenvalue for constant flux boundary condition
$\phi(N_{Sh_w})$ = ratio of asymptotic fluid-side Sherwood number at finite N_{Sh_w} to value for $N_{Sh_w} = \infty$
$\phi'(x, N_{Sh_w})$ = quantity defined by Equation (67)
$\psi(m, N_{Sh_w})$ = quantity defined by Equation (30)
ξ = quantity defined by Equation (38)
θ = dimensionless concentration, $(c - c_0)/(c_i - c_0)$
ω = dimensionless coordinate, $\frac{1}{2} - y$
χ = quantity defined by Equation (48)

Subscripts

i = initial
f = fluid-side
m = mixing cup mean; index of eigenvalues
o = overall; outside wall
w = wall (evaluated at $y = \frac{1}{2}$ or $\eta = 0$)

LITERATURE CITED

1. Graetz, L., *Ann. Physik*, **25**, 337 (1885).
2. Jakob, M., "Heat Transfer, Vol. I," p. 451, John Wiley & Sons, New York, (1949).
3. Brown, G. M., *AIChE J.*, **6**, 179 (1960).
4. Van der Does De Bye, J.A.W., and J. Schenk, *Appl. Sci. Res., Sect. A.*, **3**, 308 (1952).
5. Grimsrud, L., and A. L. Babb, *Chem. Eng. Progr. Symp. Ser. No. 66*, **62**, 19 (1966).
6. Schenk, J., *Appl. Sci. Res., Sect. A.*, **4**, 222 (1954).
7. ———, *ibid.*, **5**, 241 (1955).
8. Schenk, J., and H. L. Beckers, *Appl. Sci. Res., Sect. A*, **4**, 405 (1954).
9. Schenk, J., and J. M. Dunmore, *ibid.*, 39 (1953).
10. Schenk, J., and J. Van Laar, *ibid.*, **7**, 449 (1957).
11. Berry, V. J., *ibid.*, **4**, 61 (1953).
12. Dennis, S. C. R., and G. Poots, *ibid.*, **5**, 453 (1956).
13. Sellars, J. R., M. Tribus, and J. S. Klein, *Trans. ASME (Am. Soc. Mech. Engrs.)*, **78**, 441 (1956).
14. Schneider, P. J., *Trans. ASME (Am. Soc. Mech. Engrs.)*, **79**, 765 (1957).
15. Eckert, E. R. G., and R. M. Drake, Jr., "Heat and Mass Transfer," McGraw-Hill Book Co., Inc., New York (1959).
16. Colton, C. K., Ph.D. thesis, Mass. Inst. Technol., Cambridge (1969).
17. Stroeve, P., S.M. thesis, Mass. Inst. Technol., Cambridge (1969).
18. Cess, R. D., and E. C. Shaffer, *Appl. Sci. Res., Sect. A*, **8**, 339 (1959).
19. Leveque, J., *Ann. Mines* (Ser. *12*), **13**, 201, 305, 381 (1928).
20. Bird, R. B., *Chem.-Ingr. Tech.*, **31**, 569-72 (1959).